Proceedings of the
5th ASME/JSME Joint Thermal Engineering Conference
March 15-19, 1999, San Diego, California

AJTE99-6511

A Molecular Dynamics Simulation of a Bubble Nucleation on Solid Surface

Shigeo MARUYAMA and Tatsuto KIMURA
Department of Mechanical Engineering
The University of Tokyo
7-3-1 Hongo, Bunkyo-ku, Tokyo 113-8656, Japan
maruyama@photon.t.u-tokyo.ac.jp

Keywords: Microscale Heat Transfer, Molecular Dynamics Method, Vapor Bubble, Heterogeneous Nucleation, Solid Surface

ABSTRACT

In order to understand the molecular level phenomena related to the phase-change heat transfer, we are performing molecular dynamics simulations of a liquid droplet and a vapor bubble. Since many of practical nucleation phenomena are on the solid surface, we are paying special attention to the effect of a solid surface. In addition to the nucleation phenomena, a microscopic droplet or a vapor are of importance when an extreme condition of heat transfer such as a droplet formation in the chemical vapor deposition process and a bubble formation due to the intense laser heating on the solid surface.

Here, a heterogeneous nucleation of a vapor bubble on a solid surface was simulated by the molecular dynamics method. Liquid argon between parallel solid surfaces was gradually expanded, until a vapor bubble was nucleated. Argon liquid was represented by 5488 Lennard-Jones molecules and each solid surface was represented by three layers of harmonic molecules with the constant temperature heat bath model using the phantom molecules out side of the three-layers. We used a quite wettable potential parameter on the top surface and changed the wettability on the bottom surface. The wettability was varied by changing the potential parameter between argon and solid molecule.

After the equilibrium of liquid between two solid surfaces was obtained, we slowly expanded the surfaces. According to the increase in volume, the decrease of pressure was observed. There appeared patches of liquid where the local potential was considerably high. These patches appeared and disappeared randomly in space and time. Finally, at some point of the decrease of the pressure, one of the patches successfully grew to a vapor bubble on the bottom solid surface (Figure A-1). Observed pressure showed the minimum at this time of the nucleation. We compared the minimum pressure for various surface potential conditions. With the increase in the surface wettability, the minimum pressure approached to the spinodal line.

After the stable vapor bubble was formed on the surface, we stopped the expansion and observed the equilibrium structure of the vapor bubble. After averaging the two-dimensional density and potential distributions, we could define the contact angle. The contact angle was well correlated to the depth of the integrated effective surface potential in excellent agreement with the case of liquid droplet in contact with the surface.

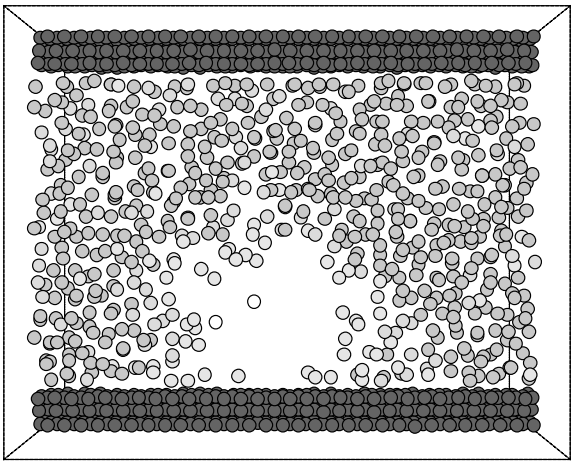

Figure A-1 A sliced snapshot of vapor bubble on solid surface.

NOMENCLEATURE

H_c : Center of fitting circle
h : Height
k : Spring constant
k_B : Boltzmann constant
m : Mass
N : Number of molecules
P : Pressure
$R_{1/2}$: Radius of fitting circle
r : Radius or distance of two molecules
r_c : Cutoff Radius
T : Temperature
V : Volume

Greek Symbols

α : Damping factor
Δt : Time step
ε : Energy parameter of Lennard-Jones potential
ϕ : Potential function
θ : Contact angle
σ : Length parameter of Lennard-Jones potential
σ_F : Standard deviation of exciting force

Subscripts

AR : Argon
DNS : Density profile
INT : Interaction between argon and solid molecules
POT : Potential profile
S : Solid molecule
SURF : Integrated for surface

INTRODUCTION

Microscopic understandings of phase interfaces have been badly anticipated in theories of traditional macroscopic heat transfer such as condensation coefficient in dropwise condensation, maximum heat transfer in boiling heat transfer, free energy of a cluster in nucleation theory, and contact angle for the heat transfer of three-phase interface. Furthermore, recent advanced technologies introduced new microscopic problems in heat transfer such as droplet formation in the chemical vapor deposition process and a vapor bubble formation due to the intense laser heating. In order to understand the molecular level phenomena related to the phase-change heat transfer, we have been performing molecular dynamics simulations of liquid-vapor interface of a liquid droplet (Maruyama et al., 1994), contact of liquid droplet on a surface (Matsumoto et al., 1995), and evaporation and condensation of liquid droplets on solid surface (Maruyama et al., 1998). In this paper, a vapor bubble nucleation on a solid surface closely related to the cavitation and boiling phenomena was considered by the molecular dynamics method.

We used simple Lennard-Jones molecules for liquid and vapor molecules and further employed the Lennard-Jones function for the interaction potential between fluid and solid molecules. The solid molecules were represented by harmonic molecules with a temperature control using the phantom molecules. By gradually expanding the solid walls to the negative pressure, we could observe the formation of vapor bubble on the surface. The dynamic behavior of liquid density fluctuations leading to the bubble formation was studied by visualizing the low density patches of liquid. Then, the equilibrium shape of the vapor bubble attached to the surface was considered. The measured contact angle was in good agreement with the case of liquid droplet in contact with the surface [Matsumoto et al. (1995), Maruyama et al. (1998)].

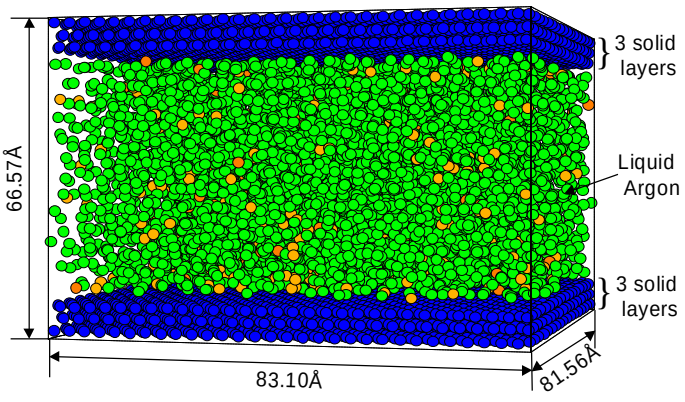

Figure 1 A snapshot of liquid argon between parallel solid surfaces.

MOLECULAR DYNAMICS SIMULATION

A heterogeneous nucleation of a vapor bubble on a solid surface was simulated by the molecular dynamics method. As shown in Figure 1, liquid argon consisted of 5488 molecules between parallel solid surfaces was prepared. The potential between argon molecules was represented by the well-known Lennard-Jones (12-6) function as

$$\phi(r) = 4\varepsilon\left\{\left(\frac{\sigma}{r}\right)^{12} - \left(\frac{\sigma}{r}\right)^{6}\right\} \qquad (1)$$

where the length scale σ_{AR} = 3.40 Å, energy scale ε_{AR} = 1.67×10^{-21} J, and mass m_{AR} = 6.63×10^{-26} kg. We used the potential cut-off at 3.5 σ_{AR} with the shift of the function for the continuous decay (Stoddard & Ford, 1973).

$$\phi_{SF}(r) = 4\varepsilon\left[\left\{\left(\frac{\sigma}{r}\right)^{12} - \left(\frac{\sigma}{r}\right)^{6}\right\} + \left\{6\left(\frac{\sigma}{r_c}\right)^{12} - 3\left(\frac{\sigma}{r_c}\right)^{6}\right\}\left(\frac{r}{r_c}\right)^{2} - \left\{7\left(\frac{\sigma}{r_c}\right)^{12} - 4\left(\frac{\sigma}{r_c}\right)^{6}\right\}\right] \quad (2)$$

Even though we could regard the system as Lennard-Jones fluid by the non-dimensional form, here we pretended that it was argon for the sake of physical understanding. The liquid argon was sandwiched by top and bottom solid surfaces, being periodic boundary conditions in four side surfaces.

The solid surface was represented by 3 layers of harmonic molecules (1020 molecules in each layer) in fcc (111) surface. Here, we set as: mass $m_S = 3.24\times10^{-27}$ kg, distance of nearest neighbor molecules $\sigma_S = 2.77$ Å, the spring constant $k = 46.8$ N/m, from the physical properties of solid platinum crystal. However, we regarded the solid as a simple insulating material because the effect of free electron and the accurate interaction potential between the metal atom and fluid atom were not explored yet. We have controlled the temperature of the solid surface by arranging a layer of phantom molecules outside of 3 layers. The phantom molecules modeled the infinitely wide bulk solid kept at a constant temperature T with proper heat conduction characteristics [Tully (1980), Blömer & Beylich (1997)]. In practice, a solid molecule in the 3rd layer was connected with a phantom molecule with a spring of 2 k and a damper of $\alpha = 5.184\text{x}10^{-12}$ kg/s in vertical direction and springs of 3.5 k and dampers of α in two horizontal directions. A phantom molecule was further excited by the random force of gaussian distribution with the standard deviation

$$\sigma_F = \sqrt{\frac{2\alpha k_B T}{\Delta t}} \quad (3)$$

where k_B is Boltzmann constant. This technique mimicked the constant temperature heat bath, which conducted heat from and to the 3rd layer as if a bulk solid was connected.

Table 1. Calculation Conditions

Label	ε_{INT} ($\times10^{-21}$J)	ε^*_{SURF}	θ_{DNS} (deg)	θ_{POT} (deg)
P2	0.467	1.65	118.7	117.1
P3	0.610	2.15	82.7	78.1
P4	0.752	2.65	60.2	53.4
P5	0.894	3.15	-	-

The potential between argon and solid molecule was also represented by the Lennard-Jones potential function with various energy scale parameter ε_{INT}. The length scale of the interaction potential σ_{INT} was kept constant as $(\sigma_S + \sigma_{AR}) / 2 = 3.085$ Å. In our previous study on the liquid droplet on the surface [Matsumoto et al. (1995), Maruyama et al. (1998)], we have found that the depth of the integrated effective surface potential ε_{SURF} was directly related to the wettability of the surface. Hence, we used a quite wettable potential parameter ($\varepsilon_{INT} = 0.894\times10^{-21}$ J) on the top surface to prevent from bubble nucleation and changed the wettability on the bottom surface as in Table 1. The solid surface became more wettable from P2 to P5.

The classical momentum equation was integrated by the Verlet's leap-frog method with the time step of 5 fs. As an initial condition, an argon fcc crystal was placed at the center of the calculation domain of $83.10 \times 81.56 \times 66.57$ Å^3 as in Figure 1. We used the velocity-scaling temperature-control toward 110 K directly to argon molecules for initial 100 ps. Then, switching off the direct temperature control, the system was run for 500 ps with the temperature control from the phantom molecules until the equilibrium argon liquid was achieved. Then, we gradually expanded the system volume by moving the top surface at a constant speed of 5 Å/ns (0.5 m/s). We could observe the bubble formation and growth. When we measured the equilibrium shape of the vapor bubble, we picked up the time where the vapor bubble was well established as the initial condition and repeated the calculation for 400 ps without the expansion of the volume.

FORMATION OF VAPOR BUBBLE

After the equilibrium of liquid between two solid surfaces at desired temperature was obtained, we slowly expanded the surfaces in the constant temperature condition imposed by phantom molecules. According to the increase in volume, the decrease of pressure was observed as in Figure 2. Here, we defined two different schemes for the evaluation of pressure. One is the direct measurement of force acting on solid surface molecules, denoted as "Wall Pressure" in Figure 2. The other is the extension of the virial representation. The virial pressure for two-body potential system is expressed as

$$PV = Nk_BT - \frac{1}{3}\sum_{i\in V}\overline{\boldsymbol{r}^i \cdot \nabla_i \phi} \quad (4)$$

where the virial internal term should be summed for all

molecule pairs inside the control volume. This summation is often extended to the outside of the periodic boundary conditions to evaluate the pressure value from a small calculation volume (Allen & Tildesley, 1987). Even though this extension to the infinite system is physically questionable (Iwaki, 1996), we applied this scheme to compare with the well defined phase diagram of Lennard-Jones system (Nicolas et al., 1979).

The pressure variation showed a broad minimum after the expansion and we could observe the formation of vapor bubble in this time range. It seemed that the pressure recovery was related to the bubble growth. In order to visualize the density variations leading to the vapor bubble nucleation, we have applied three-dimensional grids of 2 Å intervals and visualized the grid as a 'void' when there were no molecules within 1.2 σ_{AR}. An example of such a void view representation is shown in Figure 3(b) in comparison with the instantaneous sliced view (Figure 3(a)) which is the well established vapor bubble. Obviously, the assemble of such voids effectively represents the real void in the liquid. We have traced fluctuations of local density with this instantaneous void view.

Figure 4 shows an example of snapshots for a moderately wettable condition (P3; see our web site for the motion picture [http://www.photon.t.u-tokyo.ac.jp/~maruyama/bubble/]). There appeared patches of liquid where the local density was considerably low. These patches appeared and disappeared randomly in space and time but preferentially near the bottom surface. Finally, one of the patches successfully grew to a stable vapor bubble on the bottom solid surface where the lower wettability helped to sustain the nucleated bubble. It seems that when the void size is as large as 100 voids (related to about the radius of 10 Å), a single stable vapor bubble stayed on the surface. Another example of the density fluctuations for more wettable surface is shown in Figure 5. Here, except for a short appearance of medium sized voids in Figure 5(c), no stable large void appeared until the sudden formation of the bubble in Figure 5(f) (see also Figure 2). It can be regarded that the bottom surface was not helpful

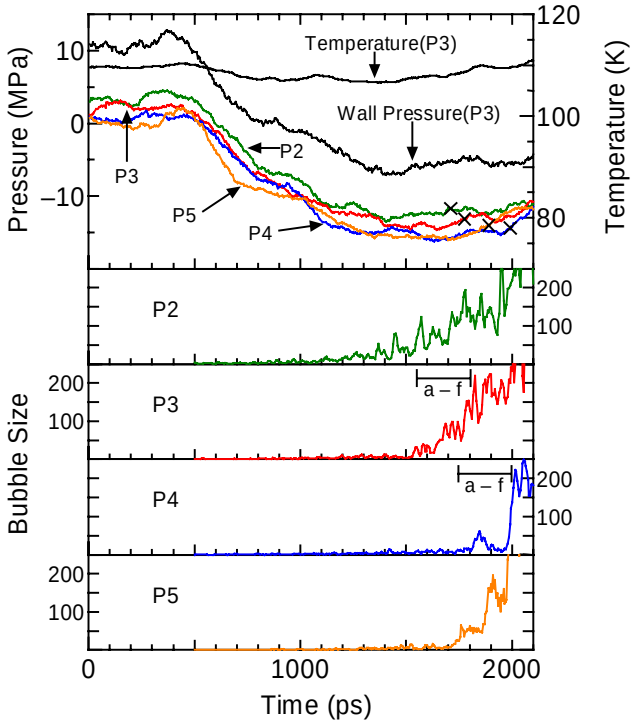

Figure 2 Pressure, temperature and bubble size variations.

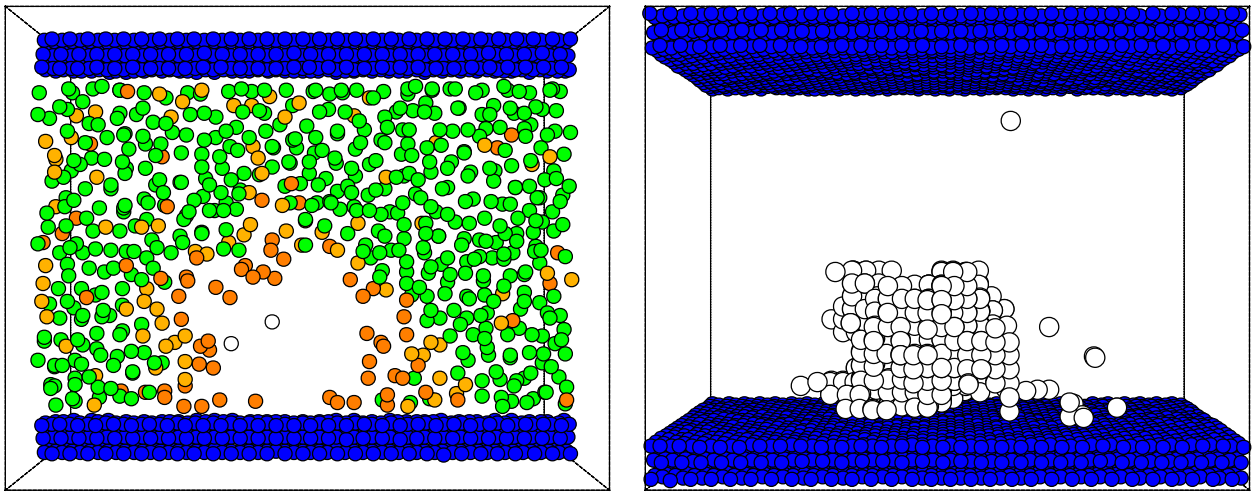

(a) Sliced View: Central 10 Å thick is shown. (b) Void View: Grids points of void are shown.

Figure 3 A snapshot of a vapor bubble at 2100 ps for P3.

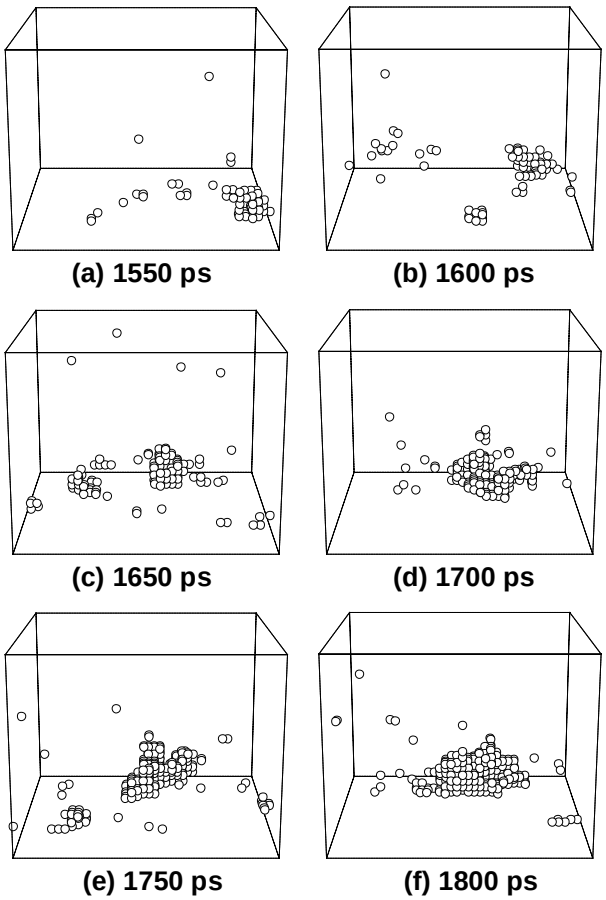

Figure 4 Snapshots of void patterns for P3.

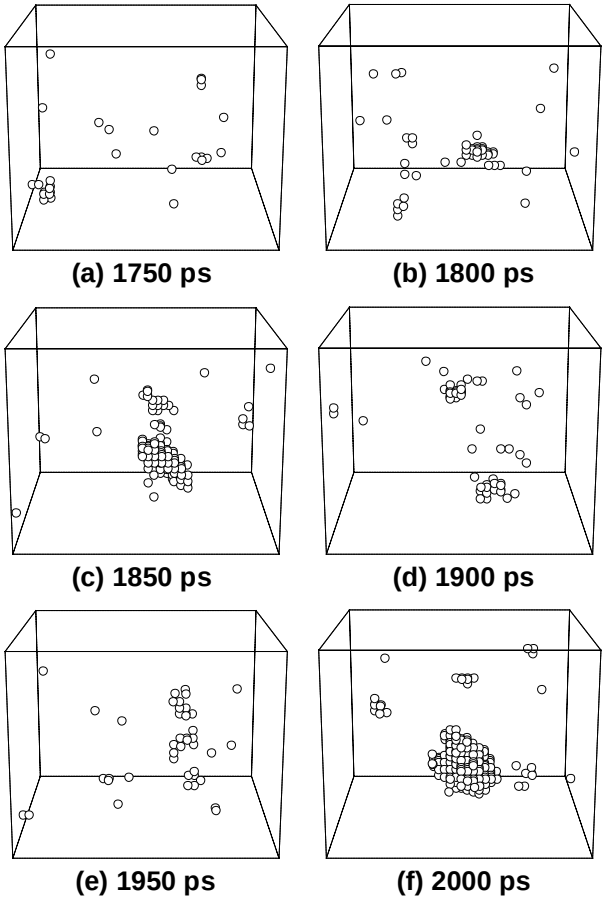

Figure 5 Snapshots of void patterns for P4 (Wettable surface).

enough to maintain the intermediate voids.

The size of the largest void in each snapshot is drawn in Figure 2 as "Bubble Size" in comparison with the pressure variations. When the bottom surface is less wettable, the size of void seems to increase monotonically, however, each void appeared and disappeared randomly in space. On the other hand, when the bottom surface is more wettable, no large void appeared until the sudden appearance of the void of about more that 100. We defined the nucleation point when the size of void exceeds 100.

We compared the nucleation pressure for various surface potential conditions (wettability) in temperature-pressure diagram in Figure 6. With the increase in the surface wettability, the nucleation pressure approached to the spinodal line (the thermodynamic limit of the existence of superheated liquid, calculated with the molecular dynamics method (Nicolas et al., 1979)). The result of the homogeneous nucleation simulation (Kinjo & Matsumoto, 1996) is also plotted in Figure 6. When a very high wettability of the surface was employed, the situation was closer to the homogeneous nucleation as for P4 and P5. With the decrease in the wettability, the nucleation point moved farther

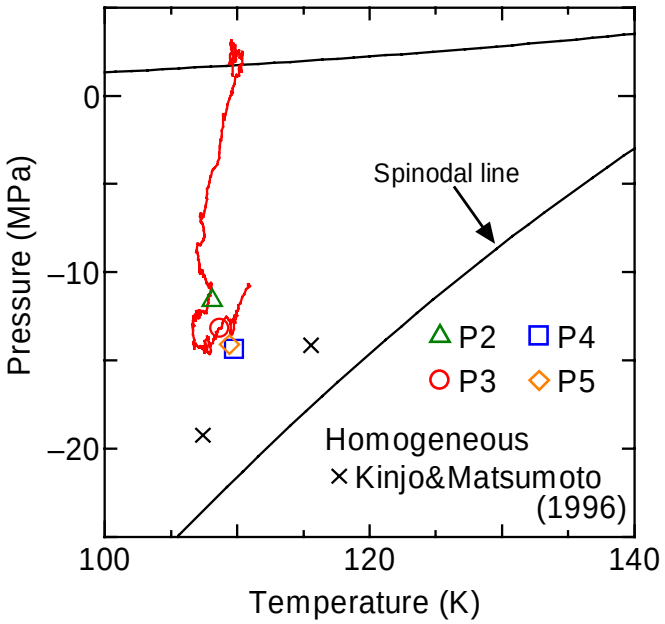

Figure 6 Temperature-Pressure diagram.

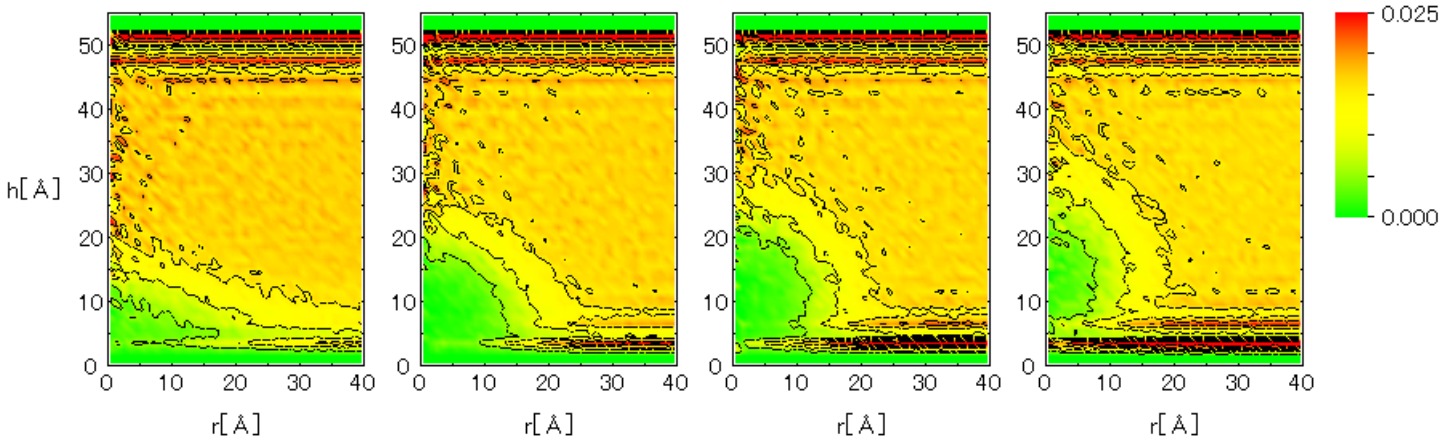

Figure 7 Two-dimensional density distributions.

from the spinodal line. These trends are very much in good agreement with the macroscopic concept that the less wettable surface helps the nucleation on the surface.

Equilibrium Shape of Vapor Bubble (Contact angle)

After detecting the stable vapor bubble formed on the surface, we repeated the simulation for 400 ps without the volume expansion in order to observe the equilibrium structure of the vapor bubble. The two-dimensional density distributions shown in Figure 7 are obtained by cylindrical averaging through the center of the bubble. The layered structure of liquid near the surface is clearly observed. On the other hand, except for about two layers near the surface the shape of bubble can be considered to be a part of a sphere. It is observed that the less wettable surface leads to more flattered shape. Compared with the density profile, the potential profile in Figure 8 had no layered structure near the liquid-solid interface. These features of the vapor bubble are just the reversed image of our previous MD simulation of a droplet near the surface as in Figure 9 (Maruyama et al., 1998). We have measured the apparent contact angle by the least square fit of a circle to the density contour line of half of liquid density. Since we have discovered that the $\cos\theta$ was a linear function of the depth of integrated effective surface potential $\varepsilon^*_{SURF} = \varepsilon_{SURF} / \varepsilon_{AR}$ for the liquid droplet on the surface (Maruyama et al., 1998), we have compared the present result with the same fashion in Figure 10. It is obvious that the contact angle was in good agreement with the case of liquid droplet marked as cross symbols [Matsumoto et al. (1995), Maruyama et al. (1998)].

It is interesting to consider the most wettable surface in Figure 7(d) (P5), in which the layered liquid structure completely covered the surface. As we monitored the position of center of bubble, it stayed at almost the same

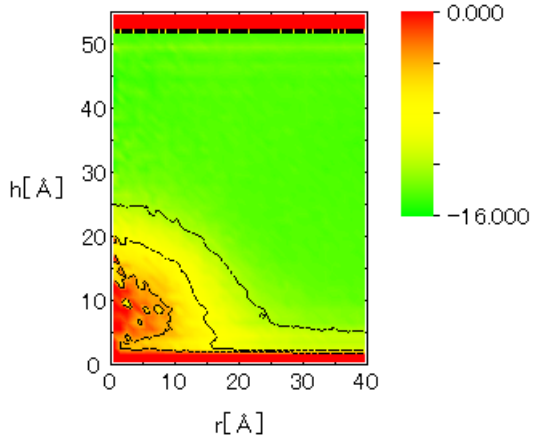

Figure 8 Two-dimensional potential distribution for P3.

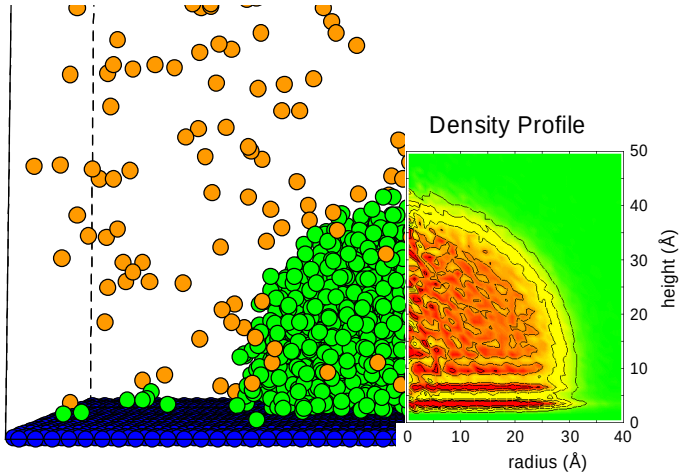

Figure 9 Snapshot compared with two-dimensional density profile for a droplet on a solid surface. N = 1944, T = 95 K, ε_{INT} = 0.575 ×10^{-21} J.

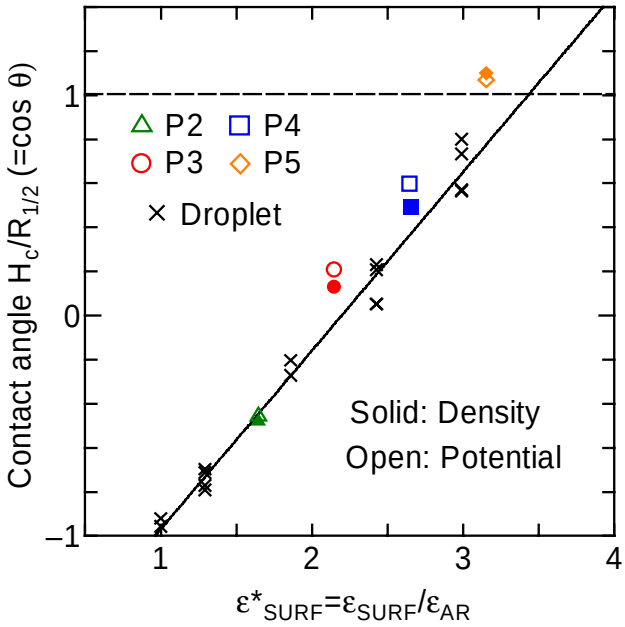

Figure 10 Contact angle correlated with ε^*_{SURF}.

height from the bottom surface, though the ε_{INT} parameter on both surfaces were the same for this condition P5. Even though the effect of the top surface might be concerned because the vertical calculation domain is limited, it is confirmed that the bubble was trapped by the bottom surface. Furthermore, if we extend the definition of the contact angle $\cos\theta$ to H_c / $R_{1/2}$, the measured point is almost on the line in Figure 10. Here, $R_{1/2}$ is the radius of the fitting circle to the half-density contour, and H_c is the center of the fitting circle. This suggests the possibility of characterizing the liquid-solid contact beyond the apparent contact angle.

CONCLUSION

We have successfully demonstrated the nucleation of a 3-dimensional vapor bubble on the solid surface using the molecular dynamics method. The equilibrium shape of the vapor bubble was characterized by the potential parameter just in the same fashion as in the liquid droplet on the solid surface. Furthermore, dynamic behaviors of the low-density patches leading to the bubble nucleation were visualized for several wettability conditions.

REFERENCES

Allen, M. P. and Tildesley, D. J., 1987, *Computer Simulation of Liquids*, Oxford University Press, Oxford.

Blömer, J. and Beylich, A. E., 1997, "MD-Simulation of Inelastic Molecular Collisions with Condensed Matter Surfaces," *Proc. 20th Int. Symp. on Rarefied Gas Dynamics*, pp. 392-397.

Iwaki, T., 1996, "Molecular Dynamics Simulation of Thermal Stress during Rapid Solidification," *Trans. JSME, Ser. A*, vol. 62-593.

Kinjo, T. and Matsumoto, M., 1996, "MD Simulation of the Inception of Vapor Phase in Lennard-Jones Luquids," *Proc. ICHMT Symp.*, vol. 1, pp. 215-221.

Maruyama, S., Matsumoto, S. and Ogita, A., 1994, "Surface Phenomena of Molecular Clusters by Molecular Dynamics Method," *Thermal Science Engineering*, vol. 2-1, pp. 77-88.

Maruyama, S., Kurashige, T., Matsumoto, S., Yamaguchi, Y. and Kimura, T., 1998, "Liquid Droplet in Contact with a Solid Surface," *Microscale Thermophysical Engineering*, vol. 2-1, pp. 49-62.

Matsumoto, S., Maruyama, S. and Saruwatari, H., 1995, "A Molecular Dynamics Simulation of a Liquid Droplet on a Solid Surface," *Proc. ASME/JSME Thermal Engineering Joint Conf.*, vol. 2, pp. 557-562.

Nicolas, J. J., Gubbins, K. E., Streett, W. B. and Tildesley, D. J., 1979, "Equation of State for the Lennard-Jones Fluid," *Molecular Physics*, vol. 37-5, pp. 1429-1454.

Stoddard, S. D. and Ford, J., 1973, "Numerical Experiments on the Stochastic Behavior of a Lennard-Jones Gas System," *Phys. Rev. A*, vol. 8, pp. 1504-1512.

Tully, J. C., 1980, "Dynamics of Gas-Surface Interactions: 3D Generalized Langevin Model Applied to fcc and bcc Surfaces," *J. Chem. Phys.*, vol. 73-4, pp. 1975-1985.